Frequency Trajectory Planning Based VSC Control Strategy for Power System Frequency Regulation

Liansong Xiong
School of Electrical Engineering
Xi'an Jiaotong University
Xi'an 710049, China
xiongliansong@163.com

Lei Liu
School of Electrical Engineering
Xi'an Jiaotong University
Xi'an 710049, China
leiliuxjtu@stu.xjtu.edu.cn

Xiaokang Liu
Department of Electronics, Information, and Bioengineering
Politecnico di Milano
Milano, Italy
xiaokang.liu@polimi.it

Yonghui Liu
School of Electrical Engineering
Xi'an Jiaotong University
Xi'an 710049, China
liuyonghui@stu.xjtu.edu.cn

***Abstract*—To ensure frequency stability of low inertia power systems, VSC needs to provide frequency response (FR) service. Limited by predicting grid inertia/damping and disturbances that are difficult to measure, the FR performance is greatly restricted. Besides, excessive response under certain conditions results in several consequences, including 1) energy waste, and 2) the VSC power frequently and excessively deviating from steady-state points, thereby reducing the component's life, lowering system safety/reliability, and increasing the risk of VSC over-current faults. To solve these issues, this paper proposes the frequency trajectory planning (FTP) based FR strategy, with the fundamental idea to actively plan the frequency trajectory with necessary safety margin in accordance with the grid code. Specifically, if the system frequency locates within the range of planned one (suggesting frequency indexes satisfying the requirement), VSC remains at the steady-state point to avoid excessive FR service; otherwise, the FR service is required, and the FTP control is enabled to closely track the planned trajectory. By fulfilling the tracking purpose, the requirement on system frequency indexes is met, frequency stability is guaranteed, and the over-response is avoided. Namely, the planned trajectory can characterize whether the system requires FR service and whether the provided FR service is sufficient or excessive. Additionally, the method needs no measurement of inertia/damping and disturbances of the system, and can be directly integrated into the commonly used VSC control systems. Finally, experiments prove the effectiveness and advancement of the FTP strategy.**

Keywords—Frequency trajectory planning, VSC, frequency stability, frequency response, low inertia power system.

I. Introduction

The short-term frequency stability is one category of the power system stability issues according to the classification in a recent technical report released by IEEE Power System Dynamic Performance Committee [1]. The frequency deviation and the rate of change of frequency (RoCoF) are two important indicators of the frequency stability, and their significant values can cause a series of adverse consequences [2]. As a common practice in many countries, the frequency-related relays will be triggered when the frequency deviation or the RoCoF exceeds the pertinent threshold regulated by the grid code, with the aim to guarantee the frequency stability [3].For instance, the frequency nadir limits specified in Ireland, Australia, United States, and Great Britain are 47.5 Hz, 47.5 Hz, 59.3 Hz (with 60 Hz-nominal frequency), and 49.5 Hz, respectively. Typical RoCoF relay settings range from 0.1 Hz/s to 1.0 Hz/s in 50 Hz power systems, and from 0.12 Hz/s to 1.2 Hz/s in 60 Hz power systems [4]

Synchronous generators (SGs) are characterized by notable frequency response (FR) features, namely, an SG can adjust its output power autonomously based on the change in grid frequency, and the FR power includes the inertia and damping powers that are proportional to frequency deviation and RoCoF, respectively. Hence, classic power systems mainly composed of SGs have excellent inertia and damping characteristics, with their frequency deviation and RoCoF easily satisfying the grid code, and frequency stability issues rarely occur. However, with large-scale application of PV and wind generation [5], STATCOM [6], electric vehicles, and electrified railways [7], power systems exhibit a high proportion of voltage source converters (VSCs) [8-9]. These VSCs, mainly utilized for transmitting desired electric power to the utility or the load, are generally viewed as constant power sources [10]. Wide application of such VSCs results in lower proportion of SGs and thus gradually weakened grid inertia. When the low-inertia power systems suffer from disturbances, their RoCoF and frequency deviation easily exceed the pertinent relay threshold, and consequently, load shedding or generator disconnection relays can be triggered [11].

To guarantee the frequency stability of low-inertia systems, many countries have compromised the RoCoF relay thresholds. Meanwhile, similar to SGs in conventional power systems, VSCs should provide adequate FR service to actively support frequency stability of low-inertia power systems. To this end, many efforts have been made to acquire sufficient FR power by equipping VSCs with various FR techniques [12], such as synchronverter and synchronous power control. Besides, the equivalence of droop control and VSG control under certain conditions is proved in [13]. With the aim to enhance system damping (D) and inertia (H) parameters equivalently, the commonly used damping control and inertia control (denoted as DH control) directly provide the FR power proportional to the frequency deviation and the RoCoF, respectively. However, due to the mismatch of inertia and other parameters in the utility grid [14], complex oscillations appear unavoidably when VSCs with fixed D and H parameters are connected to the grid integrated with physical SGs. To alleviate the oscillations, various novel strategies with alternating D and H are proposed, including the alternating H scheme, the fuzzy VSG, the self-adaptive VSG, and the optimal VSG. Obtaining the optimal time-variant DH parameters generally requires the information of the random disturbances and the system inherent DH parameters that are both time-variant and cannot be detected in real time [15]. The difficulties in evaluating the deficiency of system inertia and damping results impede the optimal DH design in advance.

In addition to the control strategy, the physical cost of the VSC (related to FR energy, FR power, and equipment life, etc.) significantly affects the frequency control performance. Current FR strategies exploit the energy from DC capacitors of VSCs [16], rotors of motors and turbines [17], PV and wind generations with operating reserves [18], grid loads with demand response, and energy storage devices [19] including batteries, supercapacitors, flywheels, etc. These energy sources for FR service are extremely limited or costly. Besides, since FR power is provided additionally by VSC systems operated at rated working condition, the VSC output power inevitably deviates from its steady-state point. Under certain conditions, serious overload issues can occur and lead to overcurrent faults. When the VSC provides FR power and energy by means of DC capacitors, batteries, and rotor kinetic energy of wind turbines, frequent FR service will cause severe DC capacitor voltage fluctuations [19], continuous battery charging / discharging, and constant acceleration / deceleration of the wind turbine. The DC voltage quality is reduced, the capacitance value is lowered, the battery life is shortened, and the mechanical fatigue of the wind turbine is accelerated. Generally, frequent and undue FR service easily leads to the overcurrent faults, quick running out of the limited energy for FR service, and negative effects on the lifetime, reliability and safety of the VSC.

Therefore, when providing FR service, the VSC should amply reduce the energy consumption, output power deviation and negative impacts on system life, reliability, safety, etc., and the FR strategy should achieve its expected performance in the absence of information including grid inertia/damping and random disturbances. To this end, this article proposes the frequency trajectory planning (FTP) based FR strategy for VSCs actively supporting the frequency stability of low inertia systems. This FR strategy actively plans the frequency trajectory exactly satisfying the grid code requirement with necessary safety margin, and forces the grid frequency to closely track the planned trajectory through FTP control. This ensures that the system frequency trajectory meets the grid code, guarantees frequency stability, and sensibly avoids the difficulties in system inertia / damping estimation and random disturbance prediction.

II. BACKGROUND OF FR SERVICE

A. Necessity of FR Service

The grid frequency f reflects the power supply and demand balance in the power system. For $f = f_{\mathrm{N}}$ (nominal frequency) and power disturbance $\Delta P_{\mathrm{g}} = 0$, the VSC generation power P equals the grid absorption power P_{g} ($P_{\mathrm{g}} = P_{\mathrm{g0}}$). For $\Delta P_{\mathrm{g}} \neq 0$, f deviates from f_{N}, followed by the simultaneous FRs from system intrinsic inertia and damping as well as from the VSC with FR power P_{FR}.

Due to the speed governors and prime movers of traditional generations with ample FR capacity cannot be enabled timely in the initial stage of system FR, and hence their actions are neglected in the initial stage (in few seconds) [20]. therefore, the system short-term FR process can be described by

$$2H_0 \frac{\mathrm{d}f}{\mathrm{d}t} = P - P_{\mathrm{g}} \tag{1}$$

where H_0 is the equivalent inertia constant of grid, P is the VSC output power, and P_{g} is the power absorbed by grid.

In the event of a power disturbance, the system frequency will deviate. The grid inherit FR characteristics, along with the FR power provided by VSC, will respond to the grid frequency change as

$$\begin{cases} P = P_0 + P_{\mathrm{FR}} \\ P_{\mathrm{g}} = \left(P_{\mathrm{g0}} + \Delta P_{\mathrm{g}}\right) - D_0\left(f_{\mathrm{N}} - f_0\right) \end{cases} \tag{2}$$

where D_0 is the equivalent damping coefficient of grid, and its larger value indicates a stronger grid FR capability.

Assuming VSC maintains constant power mode during a large disturbance and provides no FR service, then substitution of (2) into (1) gives the pertinent natural system frequency as

$$f_{\mathrm{NO}} = f_0 - \frac{\Delta P_{\mathrm{g}}}{D_0}\left(1 - e^{-\frac{D_0}{2H_0}t}\right) \tag{3}$$

In such a case, the frequency deviation and RoCoF are

$$\begin{cases} \Delta f_{\mathrm{NO}} = f_{\mathrm{N}} - f_{\mathrm{NO}} = f_{\mathrm{N}} - f_0 + \dfrac{\Delta P_{\mathrm{g}}}{D_0}\left(1 - e^{-\frac{D_0}{2H_0}t}\right) \\ R_{\mathrm{NO}} = \dfrac{\mathrm{d}f_{\mathrm{NO}}}{\mathrm{d}t} = -\dfrac{\Delta P_{\mathrm{g}}}{2H_0} e^{-\frac{D_0}{2H_0}t} \end{cases} \tag{4}$$

The pertinent maxima of Δf and RoCoF are

$$\begin{cases} \left|\Delta f_{\mathrm{NO}}\right|_{\max} = \lim\limits_{t\to\infty}\left|\Delta f_{\mathrm{NO}}\right| = \left|\dfrac{\Delta P_{\mathrm{g}} + D_0\left(f_{\mathrm{N}} - f_0\right)}{D_0}\right| \\ \left|R_{\mathrm{NO}}\right|_{\max} = \lim\limits_{t\to 0}\left|R_{\mathrm{NO}}\right| = \left|\dfrac{\Delta P_{\mathrm{g}}}{2H_0}\right| \end{cases} \tag{5}$$

The disturbance inevitably introduces frequency deviation and RoCoF issues. Under the same disturbance ΔP_{g}, smaller D_0 and H_0 indicates a higher risk that Δf and RoCoF exceed the limits. In such a case, frequency deviation and RoCoF in a low inertia and weak damping system easily exceed the protection threshold set by the grid code. To reduce the maxima of Δf and RoCoF, VSCs can no longer work in constant power mode, and are required to timely provide sufficient FR power and actively support the system frequency stability.

B. Classic FR Strategy: Inertia/Damping based Schemes

Classic inertia/damping based FR schemes are focused on equivalently increasing the system inertia coefficient H and/or damping coefficient D. The pertinent FR power provided by VSCs is generally proportional to Δf and/or RoCoF, yielding

$$P_{\mathrm{FR}} = P_{\mathrm{DH}} = \left(D + sH\right)\left(f_{\mathrm{N}} - f\right) \tag{6}$$

where D and H are gains of inertia and damping controllers, respectively.

Such an FR scheme successfully interweaves inertia and damping controllers, and is denoted as a DH controller. Since the DH controller can simultaneously improve system inertia and damping features, massive FR schemes can be represented by the DH control. Thus, this work only concentrates on the DH control for FR performance and power analysis.

Substituting (6) into (2) gives the system frequency dynamic equation when the DH control is adopted, yielding

$$H_{\text{sum}}\frac{\mathrm{d}f_{\text{DH}}}{\mathrm{d}t}=Df_{\text{N}}+D_0 f_0-D_{\text{sum}} f_{\text{DH}}-\Delta P_{\text{g}} \tag{7}$$

where D_{sum} and H_{sum} represent the grid equivalent damping and inertia coefficients with DH control, respectively, and

$$\begin{cases} D_{\text{sum}}=D_0+D \\ H_{\text{sum}}=2H_0+H \end{cases} \tag{8}$$

By solving (7), the system frequency dynamics, and the maxima of Δf and RoCoF can be obtained as

$$f_{\text{DH}}=f_0-\frac{\Delta P_{\text{g}}-D\left(f_{\text{N}}-f_0\right)}{D_{\text{sum}}}\left(1-e^{-\frac{D_{\text{sum}}}{H_{\text{sum}}}t}\right) \tag{9}$$

$$\begin{cases} \left|\Delta f_{\text{DH}}\right|_{\max}=\lim\limits_{t\to\infty}\left|f_{\text{N}}-f_{\text{DH}}\right|=\dfrac{\left|\Delta P_{\text{g}}+D_0\left(f_{\text{N}}-f_0\right)\right|}{D_{\text{sum}}} \\ \left|R_{\text{DH}}\right|_{\max}=\lim\limits_{t\to 0}\left|\dfrac{\mathrm{d}f_{\text{DH}}}{\mathrm{d}t}\right|=\dfrac{\left|\Delta P_{\text{g}}-D\left(f_{\text{N}}-f_0\right)\right|}{H_{\text{sum}}} \end{cases} \tag{10}$$

Obviously, Δf and RoCoF are effectively improved by the DH control. To avoid the frequency related relays from being triggered, the FR service should assure

$$\begin{cases} \left|\Delta f_{\text{DH}}\right|_{\max}\le F_{\text{cr}} \\ \left|R_{\text{DH}}\right|_{\max}\le R_{\text{cr}} \end{cases} \tag{11}$$

where F_{cr} and R_{cr} are the thresholds of frequency deviation and RoCoF relays specified by grid code, respectively.

By substituting (10) into (11), the value ranges of DH control parameters can be obtained as

$$\begin{cases} D\ge\dfrac{\left|\Delta P_{\text{g}}+D_0\left(f_{\text{N}}-f_0\right)\right|}{F_{\text{cr}}}-D_0\triangleq D_{\text{cr}} \\ H\ge\dfrac{\left|\Delta P_{\text{g}}-D\left(f_{\text{N}}-f_0\right)\right|}{R_{\text{cr}}}-2H_0\triangleq H_{\text{cr}} \end{cases} \tag{12}$$

where D_{cr} and H_{cr} are critical DH parameters to avoid triggering frequency relays.

Besides, by substituting (12) into (6), FR power provided by the VSC under DH control can be obtained as

$$\begin{aligned} P_{\text{FR}}=P_{\text{DH}}&=\frac{D}{D_{\text{sum}}}\left[\Delta P_{\text{g}}+D_0\left(f_{\text{N}}-f_0\right)\right] \\ &+\left(\frac{H}{H_{\text{sum}}}-\frac{D}{D_{\text{sum}}}\right)\left[\Delta P_{\text{g}}-D\left(f_{\text{N}}-f_0\right)\right]e^{-\frac{D_{\text{sum}}}{H_{\text{sum}}}t} \end{aligned} \tag{13}$$

Hence, the maximum FR power provided by VSC is

$$P_{\text{DH}}\big|_{\max}=\begin{cases} \lim\limits_{t\to 0}P_{\text{DH}}=\dfrac{H\Delta P_{\text{g}}+2DH_0\left(f_{\text{N}}-f_0\right)}{H_{\text{sum}}} & \dfrac{D}{H}\le\dfrac{D_0}{2H_0} \\ \lim\limits_{t\to\infty}P_{\text{DH}}=\dfrac{D\left[\Delta P_{\text{g}}+D_0\left(f_{\text{N}}-f_0\right)\right]}{D_{\text{sum}}} & \dfrac{D}{H}\ge\dfrac{D_0}{2H_0} \end{cases} \tag{14}$$

Hence, albeit large DH controller gains increase the system equivalent inertia and damping coefficients and enhance system frequency stability, they require additional injection (or reduction) of the VSC output power w.r.t. the actual generation power and. Besides, the VSC is required to equip with ample energy reserve and must be designed with adequate capacity and overloading ability to meet the FR service requirement.

C. Main Challenges of Existing FR Strategies

As discussed, the performance and DH parameters are positively correlated with the available energy and capacity of VSC. To significantly reduce the frequency deviation and RoCoF through the FR service provided by VSC, DH parameters must be moderately enlarged. This requires ample capacity and energy for FR service, which come at a high cost.

Hence, under the premise that frequency relays are not triggered, VSC providing FR service should minimize its power deviation w.r.t. the steady-state point, thereby lowering the energy consumption. In this respect, the optimal FR service can be achieved, if the maximum FR power reaches its minimum under the constraints of (11) and (12). This can be done by adopting D_{cr} and H_{cr}, yielding

$$\min\left\{P_{\text{DH}}\big|_{\max}\right\}=\begin{cases} \dfrac{H_{\text{cr}}\Delta P_{\text{g}}+2D_{\text{cr}}H_0\left(f_{\text{N}}-f_0\right)}{H_{\text{cr}}+2H_0} & \dfrac{D_{\text{cr}}}{H_{\text{cr}}}\le\dfrac{D_0}{2H_0} \\ \dfrac{D_{\text{cr}}\left[\Delta P_{\text{g}}+D_0\left(f_{\text{N}}-f_0\right)\right]}{D_{\text{cr}}+D_0} & \dfrac{D_{\text{cr}}}{H_{\text{cr}}}\ge\dfrac{D_0}{2H_0} \end{cases} \tag{15}$$

However, the D_{cr} and H_{cr} involve several parameters that are difficult to determine preliminarily, including H_0, D_0, and ΔP_{g}. Besides, these parameters vary with time. Therefore, the low-cost, optimal operation of FR service is rarely achieved.

In response to the above challenges, an FTP based FR strategy is proposed, which assures the optimal operation of FR service provided by VSC, by approximately approaching the minimum cost while satisfying the constraints.

III. FTP Based FR Strategy

A. Basic Principles

When DH parameters take D_{cr} and H_{cr}, respectively, the critical system frequency f_{cr} that satisfies the FR service constraints is obtained by (9) as

$$f_{\text{cr}}=f_0-\frac{\Delta P_{\text{g}}-D_{\text{cr}}\left(f_{\text{N}}-f_0\right)}{D_{\text{cr}}+D_0}\left(1-e^{-\frac{D_{\text{cr}}+D_0}{H_{\text{cr}}+2H_0}t}\right) \tag{16}$$

The frequency trajectory plane is divided into 4 regions (see Fig. 1) according to D_{cr} and H_{cr} .When the system experiences a frequency drop process., 4 frequency trajectories, i.e., f_{NO}, f_{D}, f_{H}, and f_{DH} can be obtained accounting for different conditions.

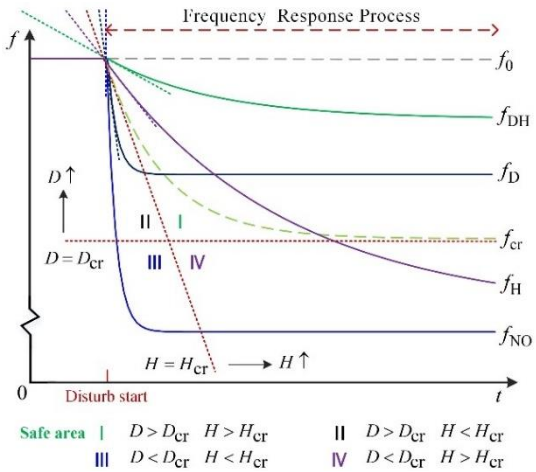

Fig. 1. System FR processes versus inertia/damping parameters.

1) Region III-insufficient inertia and damping

Without FR service provided by VSC, frequency trajectory f_{NO} can easily cross Regions II, III, and IV successively in the event of a large disturbance. In the illustrated case, f_{NO} is constantly lower than f_{cr}, causing violation of the frequency deviation and RoCoF constraints. This indicates insufficient inertia and damping. As a result, the VSC must provide FR service to enhance the system inertia and damping, such that f is constantly higher than f_{cr} and relay triggering is avoided.

2) Region IV-insufficient damping

When the inertia control is applied, the drop rate of the system frequency trajectory f_{H} decreases. If $H > H_{\mathrm{cr}}$, f_{H} completely avoids the low inertia regions (Regions II, III). However, f_{H} is still lower than f_{cr} in the final stage, namely, the frequency deviation fails to meet the constraint, indicating an insufficient damping. Accordingly, VSC needs to provide FR service and enhance the system damping, such that f is completely higher than f_{cr}. Besides, if f_{NO} avoids the low inertia regions initially, the system intrinsic inertia is sufficient, and the FR control can set null H parameter to save the available energy and capacity.

3) Region II-insufficient inertia

Similarly, when the damping control is applied, frequency deviation of f_{D} is weakened. If $> D_{\mathrm{cr}}$, f_{D} completely avoids the weak damping regions (Regions III, IV), i.e., the frequency deviation satisfies the constraint. However, f_{D} is still lower than f_{cr} in the initial stage, indicating violation of the RoCoF constraint and insufficient inertia. Hence, the VSC is required to provide FR service and enhance the system inertia, such that f is completely larger than f_{cr}. Besides, if f_{NO} avoids weak damping regions, the system damping is sufficient, and the D parameter can be null.

4) Region I-sufficient inertia and damping

When DH controls are adopted simultaneously, frequency deviation and RoCoF of f_{DH} are effectively suppressed. If D and H are greater than D_{cr} and H_{cr}, respectively, f_{DH} avoids the low inertia/weak damping regions and is always higher than f_{cr}. In such a case, the frequency deviation and RoCoF meet the constraints, suggesting sufficient and effective FR service provided by VSC. Besides, if f_{NO} is constrained in Region I, FR service from VSC is unnecessary.

Based on the above analysis, the DH control confines the system frequency trajectory within the safety region ($D > D_{cr}$ and $H > H_{cr}$ in Fig. 1) as its operation target. If the system can operate autonomously in the safety domain, the VSC does not provide FR service; otherwise, the FR service from VSC must be enabled timely to constrain the system frequency, and f_{cr} is the final objective to achieve.

In light of this, the FR strategy in this work directly defines its target as imposing the evolution of system frequency within f_{cr}, such that minimum FR energy and power are consumed, yet avoiding triggering frequency relays. This equivalently achieves the effect of the DH control with D_{cr} and H_{cr}.

B. Critical Frequency Trajectory Expression

To preliminarily determine the FR control target, i.e., f_{cr}, the unknown parameters D_0, H_0, ΔP_{g}, D_{cr} and H_{cr}, must be removed. To this end, four evolutionary dynamics of system frequency can be identified as shown in Fig. 2.

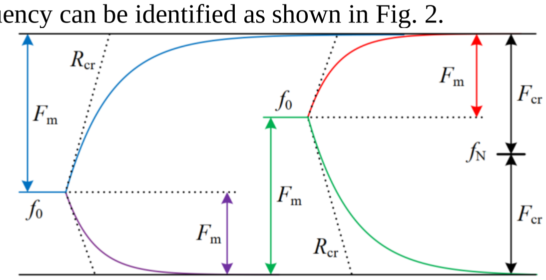

Fig. 2. Evolutionary trends of the system frequency trajectory.

The direction of the disturbance determines the sign of system RoCoF $R = df/dt$, namely, if $\Delta P_{\mathrm{g}} > 0$, then $R < 0$; conversely, if $\Delta P_{\mathrm{g}} < 0$, then $R > 0$. By substituting (8) into (7), D can be eliminated as

$$H_{\mathrm{sum}} \frac{\mathrm{d}f_{\mathrm{DH}}}{\mathrm{d}t} = D_{\mathrm{sum}} \left(f_{\mathrm{N}} - f_{\mathrm{DH}} \right) - \left[\Delta P_{\mathrm{g}} + D_0 \left(f_{\mathrm{N}} - f_0 \right) \right] \quad (17)$$

Similarly, D_0 in (7) can be eliminated, yielding

$$H_{\mathrm{sum}} \frac{\mathrm{d}f_{\mathrm{DH}}}{\mathrm{d}t} = D_{\mathrm{sum}} \left(f_0 - f_{\mathrm{DH}} \right) - \left[\Delta P_{\mathrm{g}} - D \left(f_{\mathrm{N}} - f_0 \right) \right] \quad (18)$$

Let $\mathrm{sign}(R) = 1$, which corresponds to the frequency increase case in Fig. 2 ($df_{\mathrm{DH}}/dt > 0$ and $f_{\mathrm{DH}} > f_0$). To ensure $df_{\mathrm{DH}}/dt > 0$ in (17) and (18), they should satisfy

$$\begin{cases} D_{\mathrm{sum}} \left(f_{\mathrm{N}} - f_{\mathrm{DH}} \right) > \Delta P_{\mathrm{g}} + D_0 \left(f_{\mathrm{N}} - f_0 \right) \\ D_{\mathrm{sum}} \left(f_0 - f_{\mathrm{DH}} \right) > \Delta P_{\mathrm{g}} - D \left(f_{\mathrm{N}} - f_0 \right) \end{cases} \quad (19)$$

To guarantee (19) is valid for either $f_{\mathrm{DH}} > f_{\mathrm{N}}$ or $f_{\mathrm{DH}} < f_{\mathrm{N}}$, there must be

$$\begin{cases} \Delta P_{\mathrm{g}} + D_0 \left(f_{\mathrm{N}} - f_0 \right) < 0 \\ \Delta P_{\mathrm{g}} - D \left(f_{\mathrm{N}} - f_0 \right) < 0 \end{cases} \quad \mathrm{sign}(R) = 1 \quad (20)$$

Analogously, when $\mathrm{sign}(R) = -1$ (corresponding to the frequency drop case in Fig. 2), we have

$$\begin{cases}\Delta P_{\mathrm{g}}+D_0\left(f_{\mathrm{N}}-f_0\right)>0\\ \Delta P_{\mathrm{g}}-D\left(f_{\mathrm{N}}-f_0\right)>0\end{cases}\quad \operatorname{sign}(R)=-1 \tag{21}$$

Therefore,

$$\begin{cases}\left|\Delta P_{\mathrm{g}}+D_0\left(f_{\mathrm{N}}-f_0\right)\right|=-\left[\Delta P_{\mathrm{g}}+D_0\left(f_{\mathrm{N}}-f_0\right)\right]\cdot\operatorname{sign}(R)\\ \left|\Delta P_{\mathrm{g}}-D\left(f_{\mathrm{N}}-f_0\right)\right|=-\left[\Delta P_{\mathrm{g}}-D\left(f_{\mathrm{N}}-f_0\right)\right]\cdot\operatorname{sign}(R)\end{cases} \tag{22}$$

Substituting D_{cr} and H_{cr} into (14) and (22) obtains

$$\begin{cases}\dfrac{D_{\mathrm{cr}}+D_0}{H_{\mathrm{cr}}+2H_0}=\dfrac{R_{\mathrm{cr}}}{F_{\mathrm{m}}}\\ \dfrac{\Delta P_{\mathrm{g}}-D_{\mathrm{cr}}\left(f_{\mathrm{N}}-f_0\right)}{D_{\mathrm{cr}}+D_0}=-F_{\mathrm{m}}\cdot\operatorname{sign}(R)\end{cases} \tag{23}$$

where F_{m} is the maximum allowable frequency deviation of FR service (see Fig. 2), and

$$F_{\mathrm{m}}=F_{\mathrm{cr}}+\left(f_{\mathrm{N}}-f_0\right)\cdot\operatorname{sign}(R) \tag{24}$$

Substituting (23) into (16) gives

$$f_{\mathrm{cr}}=f_0+F_{\mathrm{m}}\left(1-e^{-R_{\mathrm{cr}}t/F_{\mathrm{m}}}\right)\cdot\operatorname{sign}(R) \tag{25}$$

Compared to (16), f_{cr} given by (25) can be determined in advance, since the involved parameters are either thresholds specified by grid code (f_{N}, F_{cr} and R_{cr}) or system operational parameters that can be measured in real time (f_0 and df/dt). By limiting the system frequency within region enclosed by f_{cr}, the FTP strategy can be developed.

C. Economic Evaluation

The FTP based FR strategy has evident advantages since it minimizes the consumption of energy and capacity while satisfying the constraints. Its advantage in terms of FR power consumption is proved below by considering $\Delta P_{\mathrm{g}}>0$ and $f_0<f_{\mathrm{N}}$. Its superiority regarding energy consumption can be similarly verified. If the system frequency strictly follows the critical trajectory, the FR power provided by VSC is

$$\begin{aligned}P_{\mathrm{cr}}=&\frac{D_{\mathrm{cr}}}{D_0+D_{\mathrm{cr}}}\left[\Delta P_{\mathrm{g}}+D_0\left(f_{\mathrm{N}}-f_0\right)\right]+\\ &\left(\frac{H_{\mathrm{cr}}}{2H_0+H_{\mathrm{cr}}}-\frac{D_{\mathrm{cr}}}{D_0+D_{\mathrm{cr}}}\right)\left[\Delta P_{\mathrm{g}}-D_{\mathrm{cr}}\left(f_{\mathrm{N}}-f_0\right)\right]e^{-\frac{D_0+D_{\mathrm{cr}}}{2H_0+H_{\mathrm{cr}}}t}\end{aligned} \tag{26}$$

Substituting (23) into (26) to replace D_{cr} and H_{cr}, we have

$$P_{\mathrm{cr}}=\Delta P_{\mathrm{g}}-D_0F_{\mathrm{m}}-\left(2H_0R_{\mathrm{cr}}-D_0F_{\mathrm{m}}\right)e^{-R_{\mathrm{cr}}t/F_{\mathrm{m}}} \tag{27}$$

For inertia or damping schemes, the FR power depends on DH parameters. Assume they are designed according to the maximum disturbance power ΔP_{gmax}, namely

$$\begin{cases}D+D_0=\dfrac{\Delta P_{\mathrm{gmax}}+D_0\left(f_{\mathrm{N}}-f_0\right)}{F_{\mathrm{cr}}}\\ H+2H_0=\dfrac{\Delta P_{\mathrm{gmax}}-D\left(f_{\mathrm{N}}-f_0\right)}{R_{\mathrm{cr}}}\end{cases} \tag{28}$$

A disturbance intensity coefficient σ is introduced to relate the actual disturbance power ΔP_{g} to ΔP_{gmax} as

$$\sigma=\Delta P_{\mathrm{g}}/\Delta P_{\mathrm{gmax}} \tag{29}$$

Substituting (29) into (28) gives the DH parameters

$$\begin{cases}D+D_0=\dfrac{\Delta P_{\mathrm{g}}+\sigma D_0\left(f_{\mathrm{N}}-f_0\right)}{\sigma F_{\mathrm{cr}}}\\ H+2H_0=\dfrac{\Delta P_{\mathrm{g}}+\sigma D_0\left(f_{\mathrm{N}}-f_0\right)}{\sigma F_{\mathrm{cr}}}\cdot\dfrac{F_{\mathrm{m}}}{R_{\mathrm{cr}}}\end{cases} \tag{30}$$

If ΔP_{g} is greater than ΔP_{gmax}, that is, $\sigma>1$, or the system inertia/damping coefficients under actual working conditions are less than their designed values H_0 and D_0, then the DH parameters designed based on (30) fail to satisfy (14), the frequency relays in system will be triggered, and the provided FR service cannot guarantee the stability. For such reasons, the following discussion is conducted within $0<\sigma\leq 1$.

By substituting (30) into (13), the additional FR power provided by VSC under DH control can be obtained a

$$\begin{aligned}P_{\mathrm{DH}}=&\Delta P_{\mathrm{g}}+\left(1-\rho\sigma\right)D_0F_{\mathrm{cr}}-D_0F_{\mathrm{m}}+\\ &\left[\left(1-\rho\sigma\right)\frac{F_{\mathrm{cr}}}{F_{\mathrm{m}}}-1\right]\left(2H_0R_{\mathrm{cr}}-D_0F_{\mathrm{m}}\right)e^{-\frac{R_{\mathrm{cr}}}{F_{\mathrm{m}}}t}\end{aligned} \tag{31}$$

Where

$$\rho=\frac{\Delta P_{\mathrm{g}}+D_0\left(f_{\mathrm{N}}-f_0\right)}{\Delta P_{\mathrm{g}}+\sigma D_0\left(f_{\mathrm{N}}-f_0\right)} \tag{32}$$

If the FTP strategy (instead of the DH strategy) is used for FR control, the saved FR power P_{save} can be obtained as

$$P_{\mathrm{save}}=P_{\mathrm{DH}}-P_{\mathrm{cr}}=\left(1-\rho\sigma\right)D_0F_{\mathrm{cr}}\left[1-\left(1-\frac{2H_0R_{\mathrm{cr}}}{D_0F_{\mathrm{m}}}\right)e^{-\frac{R_{\mathrm{cr}}}{F_{\mathrm{m}}}t}\right] \tag{33}$$

Fig. 3 demonstrates the dependency of P_{save} on the system frequency before disturbance (f_0), and on the disturbance intensity (σ). The benefit of the FTP method gradually grows with the FR service duration, which is more evident with larger f_0 and lower σ. Indeed, most frequently both the disturbance and preliminary frequency deviation are small, resulting in evident superiority of the FTP method.

$$P_{\mathrm{save}}\big|_{\mathrm{max}}=\begin{cases}\lim\limits_{t\to 0}P_{\mathrm{save}}=2\left(1-\rho\sigma\right)H_0R_{\mathrm{cr}}\dfrac{F_{\mathrm{cr}}}{F_{\mathrm{m}}} & \dfrac{R_{\mathrm{cr}}}{F_{\mathrm{m}}}\geq\dfrac{D_0}{2H_0}\\ \lim\limits_{t\to\infty}P_{\mathrm{save}}=\left(1-\rho\sigma\right)D_0F_{\mathrm{cr}} & \dfrac{R_{\mathrm{cr}}}{F_{\mathrm{m}}}\leq\dfrac{D_0}{2H_0}\end{cases} \tag{34}$$

The maximum P_{save} is related to H_0, D_0, and σ, as shown in Fig. 3. Besides, this advantage increases with H_0 and D_0. Indeed, for the same ΔP_{g}, the required inertia and damping to maintain certain frequency deviation and RoCoF are consistent. Larger H_0 and D_0 suggest smaller inertia/damping deficiency of the system, hence less support required for VSC, and less power/energy consumption. However, since DH control with fixed parameters provides the system constant inertia/damping that cannot be flexibly adjusted based on the needs, either the provided FR service is insufficient and the frequency related relays are triggered, or the inertia/damping provided by VSC is too much and H_0/D_0 of the system itself cannot be fully utilized. In the latter case, the extremely limited capacity and energy are wasted on FR service. This limitation is overcome by the FTP based method, with which VSC provides exactly the insufficient inertia/damping needed for FR service and facilitates retaining grid frequency stability, thereby avoiding excessive energy consumption, and minimizing the impact of FR service on the normal operation and reliability of VSC.

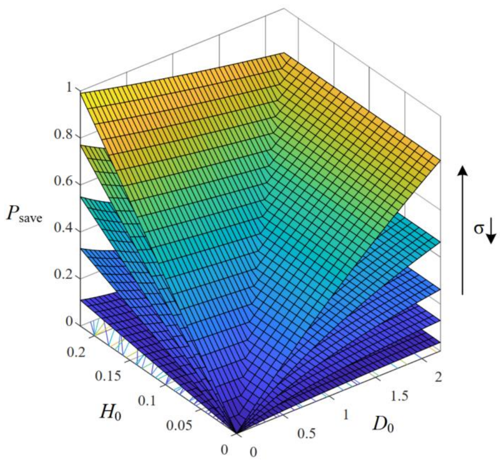

Fig. 3. Saved FR power versus system inertia and damping.

IV. Implementation of Proposed FTP Strategy

Fig. 4 shows the proposed FTP based FR strategy that contains a PLL [21], a trigger criterion, an FTP, a PD based frequency control and PI based current control [22]. f is the grid frequency detected by PLL; f_{tp} is the planned frequency curve; P and D controllers adjust the damping and inertia provided by VSC, respectively.

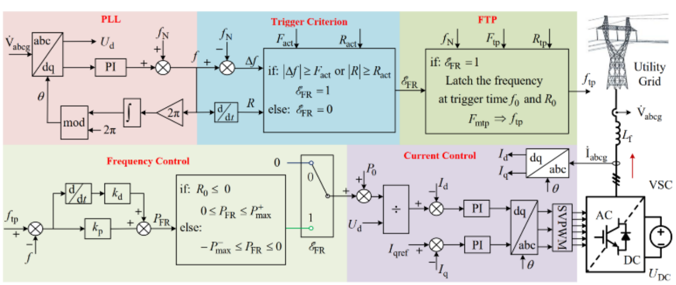

Fig. 4. FTP based VSC control strategy.

A. Frequency Trajectory Planning

It is noted that f_{cr} is the bottom line for system safe operation. Due to the control error, it is inappropriate to directly set f_{cr} as the planned trajectory of the FTP method, f_{tp}. To assure that neither f_{tp} nor f exceeds the safety range defined by f_{cr}, more stringent planning parameters F_{tp} and R_{tp} are utilized instead of F_{cr} and R_{cr} to construct f_{tp}, such that necessary safety margins F_{mar} and R_{mar} are reserved, yielding

$$\begin{cases} F_{mar} = F_{cr} - F_{tp} \\ R_{mar} = R_{cr} - R_{tp} \end{cases} \tag{35}$$

Besides, the FR service must be started prior to the frequency deviation and RoCoF reach F_{tp} and R_{tp}; otherwise, F_{mar} and R_{mar} can be exhausted. Considering the action parameters to be F_{act} and R_{act}, the FTP triggering criterion is given by

$$\varepsilon_{FR} = \begin{cases} 1 & \left(|\Delta f| \ge F_{act}\right) \cup \left(|R| \ge R_{act}\right) \\ 0 & \left(|\Delta f| < F_{act}\right) \cap \left(|R| < R_{act}\right) \end{cases} \tag{35}$$

where $\varepsilon_{FR} = 1$ enables the frequency control.

Therefore, f_{tp} can be determined as

$$f_{tp} = f_0 + F_{mtp}\left(1 - e^{-\frac{R_{tp}}{F_{mtp}}t}\right) \cdot \mathrm{sign}(R_0) \tag{36}$$

where f_0 and R_0 are the initial grid frequency and RoCoF values latched as ε_{FR} switches from 0 to 1, and F_{mpt} is the maximum allowable frequency deviation for FTP given by

$$F_{mtp} = F_{tp} + (f_N - f_0) \cdot \mathrm{sign}(R_0) \tag{37}$$

f_{tp} in (38) can be determined in advance, and the involved parameters only include planning parameters (F_{tp},R_{tp}), grid frequency information (f_0, R_0) that can be directly measured by PLL [23]. This completely avoids the technical issues of DH controls. Furthermore, the control target of minimum FR energy is achieved under the premise of frequency stability.

B. Frequency Trajectory Partitioning

Three sets of parameters involved in FTP method, namely, F_{act} and R_{act}, F_{tp} and R_{tp}, F_{cr} and R_{cr}, determine 3 boundary lines on the potential frequency trajectory plane, encompassing the FTP action line, the planning line and the relays threshold line. The frequency plane is accordingly divided into 4 regions, i.e. the safety region, the supervision region, the regulation region, and the forbidden region. In the following analysis, $\Delta P_g > 0$ is considered as an example. Its frequency trajectory is partitioned in Fig. 5.

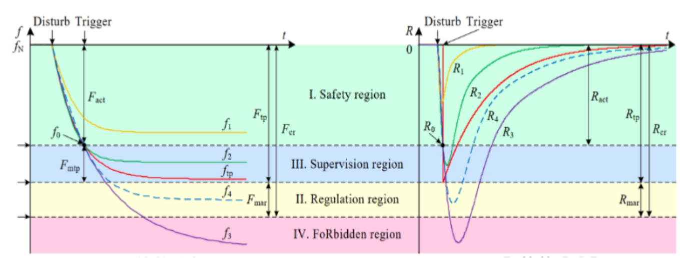

Fig. 5. Frequency partitioning of the proposed FTP method.

Safety region: In this region, the frequency deviation and RoCoF are sufficiently smaller than F_{cr} and R_{cr}, and the frequency stability is satisfactory. As an example, f_1 and R_1 are constantly located in this region, indicating a less disturbed system condition, or sufficient intrinsic inertia / damping to constrain the frequency. In this case, there is no need for VSC to provide FR service, and VSC maintains its normal operating without consuming extra energy and capacity. In fact, the system commonly faces various small disturbances that can be managed by the intrinsic inertia and damping efficiently, where the FR service is unnecessary.

Supervision region: With the further increase of disturbance, the intrinsic inertia and damping become weak in restraining the frequency deviation or RoCoF. f will enter the supervision region, and finally terminate in this region (see f_2 and R_2) or move beyond (e.g., see f_3 and R_3). Though frequency related relays will not trigger in the former case, the latter case faces a greater risk, namely, either the safety margin to $F_{\rm cr}$ and $R_{\rm cr}$ is consumed, or frequency relays are triggered as frequency enters the forbidden region (f_3 and R_3). Since both scenarios are possible, the control system must preliminarily determine the safety of grid frequency trajectory and take proper measures. This is done by comparing f with $f_{\rm tp}$, and the main role of FTP module at this time is to monitor the frequency trace. If f does not cross $f_{\rm tp}$, then it terminates in the supervision area (f_2 and R_2), and the FR service is unnecessary. Otherwise, f crossing $f_{\rm tp}$ will enter the regulation region.

Regulation region: After f enters the regulation region, part of the safety margins will be consumed, yet the relays triggering thresholds are not reached. Though the final result is still allowable, the inadequate margins $F_{\rm mar}$ and $R_{\rm mar}$ suggest insufficient system intrinsic inertia and damping to constrain f in the safety (or supervision) region. In this case, the FTP function is triggered, and the PD controller immediately outputs the FR power command and provides additional support to the system, with the aim to limit the maximum frequency deviation and RoCoF as close as possible to the planned values and to reduce the consumption of safety margins. If the system lacks sufficient intrinsic inertia/damping and also additional support, then f will pass over the regulation region and reach the forbidden region.

Forbidden region: f arriving at this region (e.g. f_3 and R_3) will trigger frequency relays and cause inevitable power outages. This suggests excessive disturbance to the system, under which the grid intrinsic inertia and damping cannot maintain its frequency stability. VSC must enable the FR service and provide sufficient inertia and damping support. To this end, the FTP function is triggered, and the PD controller immediately outputs the FR power command $P_{\rm TP}$ to raise the frequency trace from f_3 to f_4. If the trajectory moves into the regulation region through FTP control, the maximum values of frequency deviation and RoCoF are away from relay thresholds $F_{\rm cr}$ and $R_{\rm cr}$. This suggests adequate support provided by VSC to the power system that ensures the frequency stability.

Therefore, whether and in which condition the FTP block is triggered depend on the combination effect of disturbance and the grid intrinsic inertia and damping, i.e., whether they are sufficient to deal with the disturbance. Additional inertia and damping are provided by VSC if f crosses $f_{\rm tp}$. As a basic rule, the FR service avoids the system frequency track from entering the forbidden region. This is reliably achieved by reasonable frequency planning and effective control.

V. VERIFICATION

Experiments are utilized to verify the proposed FR strategy [23]. A droop control converter (see [11] for detailed information) is utilized to emulate the utility grid. Two DH controllers with different gains, denoted as large DH control and small DH control (see Table 2 for detailed parameters) hereinafter, are chosen for performance comparisons. Besides, the VSC steady-state power is 15 kW for the experiments.

In the experiment, the low inertia system experiences two disturbances in the same direction, i.e. i) a sudden increase of load power by 0.8 kW (small disturbance), and ii) another load power increase by 8 kW (large disturbance). The pertinent FR results are shown in Fig. 6. Under the consecutive disturbances, without FR service, the system frequency nadir drops to 49.3 Hz and the maximum RoCoF reaches 4.7 Hz/s during the large disturbance. Both the indicators exceed their relay thresholds, triggering the under-frequency and over-RoCoF relays. The system cannot maintain frequency stability on its own, causing partial power outages of the load. When VSC provides FR service with either strategy, the frequency deviation and RoCoF indicators are significantly reduced. This proves the significance of timely and effective FR service on improving the frequency stability of low inertia power systems.

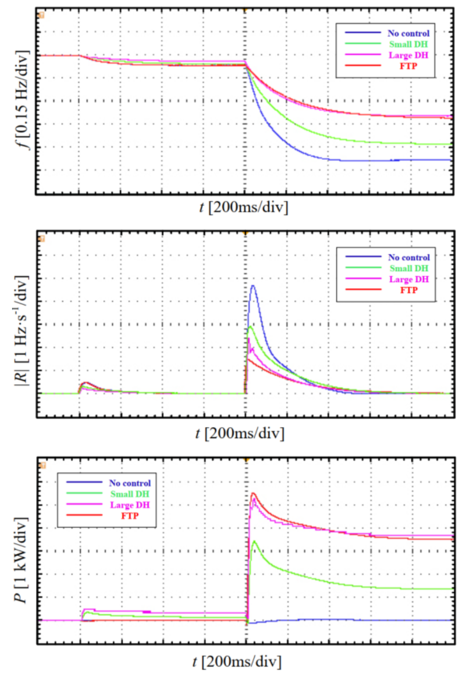

Fig. 6. FR results of power system with disturbances.

The experiment results also reveal the important differences in FR performance under three strategies. When the small DH control is used for FR service, though the maximum frequency deviation and RoCoF fall to 0.57 Hz and 3.0 Hz/s respectively, they remain slightly higher than the limits of 0.5 Hz and 2.5 Hz/s. By adopting the large DH based FR service, albeit the VSC power exhibits insignificant oscillations, the maximum frequency deviation and RoCoF are reduced to 0.39 Hz and 2.4 Hz/s, respectively, and thus achieving frequency stability. Increase in DH controller gains enhances the system equivalent inertia and damping, and hence the ability to restrain frequency deviation and RoCoF. However, when the DH controller gains are exaggerated, the oscillation becomes severe. As shown in Fig. 7, when D and H are increased to 25 and 7, respectively (denoted as ultra DH control), obvious oscillations are present in the VSC power, system frequency and RoCoF. If DH parameters further increase, the system will lose stability.

Using the FTP scheme, VSC can completely determine whether to provide FR service and the amount of provided inertia/damping according to the actual needs of power system, to achieve the minimum energy consumption. As shown in Fig. 8, when the small disturbance is applied, the maximum frequency deviation (0.06 Hz) and RoCoF (0.48 Hz/s) are smaller than the action thresholds (0.1 Hz and 0.5 Hz/s) for triggering FTP, namely, a small disturbance will not cause obvious frequency deviation and RoCoF, and the grid intrinsic inertia and damping can effectively maintain the frequency stability without the need of FR service from VSC. In this case, the VSC power, the grid frequency, and the RoCoF waveforms are fully consistent with the system natural response, indicating the proposed FTP strategy realized the accurate identification of system state and the operation of control logic. Namely, when the system does not need inertia or damping support, the FTP does not trigger, and VSC does not provide FR service.

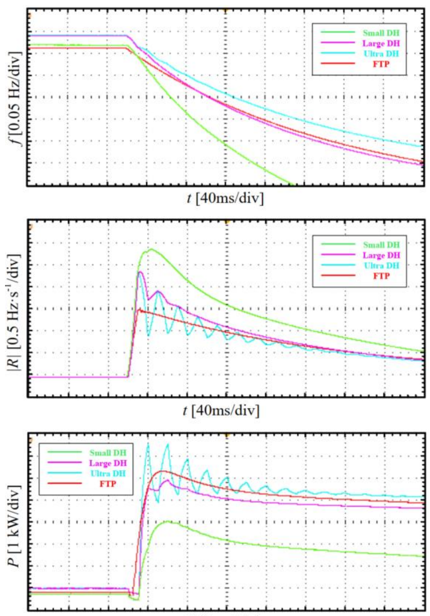

Fig. 7. FR results of power system with the large disturbance.

However, when the disturbance increases to 8 kW, due to the weak inertia, the RoCoF rapidly reaches the action threshold (0.5 Hz/s). The FTP module then plans f_{tp}, which is used by the control system as reference of system frequency. The maximum frequency deviation and RoCoF of the controlled system have dropped to 0.42 Hz and 1.5 Hz/s, respectively. Oscillations are also avoided. The results prove that the FTP strategy can actively identify whether the system needs inertia and damping support, and provide the appropriate FR service when needed. The whole FR process is stable, avoiding the oscillation issue of the large DH control. The frequency stability is achieved under experiment conditions.

The advantage is more prevailing when considering the FR power and energy costs, as shown in Fig. 8(c). Although the large DH based FR service also achieves frequency stability in this condition, the pertinent FR power is significantly higher, especially for the steady-state (which determines the energy consumption). In this case, the VSC significantly deviates from the steady-state point, thereby causing a greater adverse effect on the reliability and safety of the equipment. Conversely, the FTP strategy not only promotes the system frequency stability, but also assures the minimum power and energy consumption.

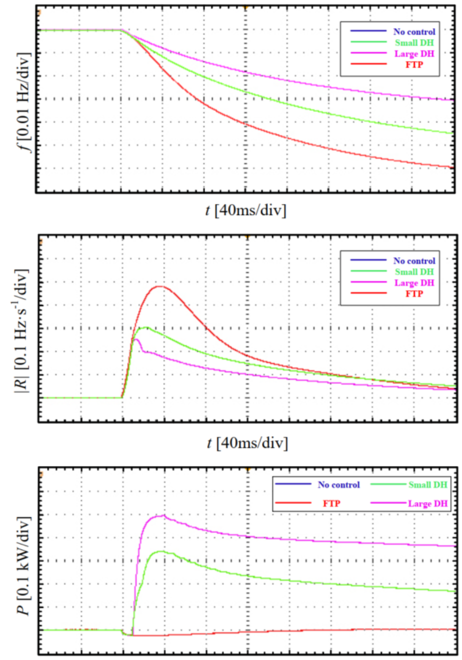

Fig. 8. FR results of power system with the small disturbance.

VI. CONCLUSION

The FTP based VSC control strategy proposed in this article actively supports the frequency stability of low inertia power systems, by restraining the frequency deviation and RoCoF within the thresholds of frequency based relays under various disturbances. The proposed strategy provides FR service only if the system frequency is out of the planned trajectory range, and only allows the system frequency to closely track the planned frequency. Accordingly, this strategy avoids excessive provision of FR service and its related problems such as energy consumption, device overload and life reduction. It is free to predict system inertia/damping and random disturbances, and can ensure the provided FR service just fulfil the needs of system frequency stability, namely, it has a wide applicability.

REFERENCES

[1] N. Hatziargyriou, J. Milanovic, C. Rahmann, et al., "Stability definitions and characterization of dynamic behavior in systems with high penetration of power electronic interfaced technologies," IEEE Power and Energy Society, Piscataway, NJ, USA, Tech. Rep., Apr. 2020, pESTR77.

[2] J. Fang, Y. Tang, H. Li, and X. Li, "A battery/ultracapacitor hybrid energy storage system for implementing the power management of virtual synchronous generators," IEEE Trans. Power Electron., vol. 33, no. 4, pp. 2820–2824, 2018.

[3] "IEEE guide for the application of protective relays used for abnormal frequency load shedding and restoration," IEEE Standard C37.117-2007, Aug. 2007.

[4] W. Freitas, W. Xu, C. Affonso, and Z. Huang, "Comparative analysis between ROCOF and vector surge relays for distributed generation applications," IEEE Trans. Power Del., vol. 20, no. 2, pp. 1315–1324, 2005.

[5] Y. Li, Z. Xu, L. Xiong, et al, "A cascading power sharing control for microgrid embedded with wind and solar generation," in Renewable Energy, vol. 132, pp. 846-860, Mar. 2019.

[6] L. Xiong, F. Zhuo and M. Zhu, "Study on the compound cascaded STATCOM and compensating for 3-phase unbalancd loads," 2013 28th Annual IEEE Applied Power Electronics Conference and Exposition, Long Beach, CA, USA, 2013, pp. 3209-3215.

[7] X. Wang, J. Liu, T. Xu, et al, "Control of a three-stage three-phase cascaded modular power electronic transformer," 2013 28th Annual IEEE Applied Power Electronics Conference and Exposition, Long Beach, CA, USA, 2013, pp. 1309-1315.

[8] L. Xiong, X. Liu, Y. Liu, and F. Zhuo, "Modeling and stability issues of voltage-source converter dominated power systems: A review," CSEE J. Power Energy Syst., pp. 1–18, 2020, doi: 10.17775/CSEEJPES.2020.03590.

[9] Y. Sun, L. Ma and L. Xiong, "A novel balancing method for DC voltage of cascaded multilevel STATCOM," 2012 Asia-Pacific Power and Energy Engineering Conference, Shanghai, China, 2012, pp. 1-5

[10] T. Liu, X. Hao, X. Yang, et al, "A novel grid voltage feed forward control strategy for three-phase grid-connected VSI with LCCL filter," 2012 IEEE International Symposium on Industrial Electronics, Hangzhou, China, 2012, pp. 86-91.

[11] L. Xiong, X. Liu, D. Zhang and Y. Liu, "Rapid power compensation based frequency response strategy for low inertia power systems," in IEEE Journal of Emerging and Selected Topics in Power Electronics, doi: 10.1109/JESTPE.2020.3032063.

[12] X. Meng, J. Liu, and Z. Liu, "A generalized droop control for grid-supporting inverter based on comparison between traditional droop control and virtual synchronous generator control," IEEE Trans. Power Electron., vol. 34, no. 6, pp. 5416–5438, 2019.

[13] S. D'Arco and J. A. Suul, "Equivalence of virtual synchronous machines and frequency-droops for converter-based MicroGrids," IEEE Trans. Smart Grid, vol. 5, no. 1, pp. 394–395, 2014.

[14] F. Wang, L. Zhang, X. Feng, and H. Guo, "An adaptive control strategy for virtual synchronous generator," IEEE Trans. Ind. Appl., vol. 54, no. 5, pp. 5124–5133, 2018.

[15] J. Schiffer, P. Aristidou, and R. Ortega, "Online estimation of power system inertia using dynamic regressor extension and mixing," IEEE Trans. Power Syst., vol. 34, no. 6, pp. 4993–5001, 2019.

[16] J. Fang, H. Li, Y. Tang, and F. Blaabjerg, "Distributed power system virtual inertia implemented by grid-connected power converters," IEEE Trans. Power Electron., vol. 33, no. 10, pp. 8488–8499, Oct. 2018.

[17] Y. Li, Z. Xu, and K. P. Wong, "Advanced control strategies of PMSG-based wind turbines for system inertia support," IEEE Trans. Power Electron., vol. 32, no. 4, pp. 3027–3037, Jul. 2017.

[18] B. Kroposki, B. Johnson, Y. Zhang, et al, "Achieving a 100% renewable grid: operating electric power systems with extremely high levels of variable renewable energy," IEEE Power Energy Mag., vol. 15, no. 2, pp. 61–73, 2017.

[19] L. Xiong, F. Zhuo, "Chopper controller based DC voltage control strategy for cascaded multilevel STATCOM," in Journal of Electrical Engineering & Technology, vol.9, no.2, pp.576-588, Mar. 2014.

[20] F. Teng, V. Trovato, and G. Strbac, "Stochastic scheduling with inertia-dependent fast frequency response requirements," IEEE Trans. Power Syst., vol. 31, no. 2, pp. 1557–1566, 2016.

[21] L. Xiong, F. Zhuo, F. Wang, et al. "A novel fast open-loop phase locking scheme based on synchronous reference frame for three-phase non-ideal power grids," in J Power Electron, vol.16, no.4, pp.1513-1525, July 2016.

[22] L. Xiong, F. Zhuo, X. Liu, et al, "Optimal design of moving average filter and its application in distorted grid synchronization," 2015 IEEE Energy Conversion Congress and Exposition, Montreal, QC, Canada, 2015, pp. 3449-3454.

[23] X. Liu, F. Zhuo, Y. Chen, et al, "Development of fast simulation models for photovoltaic generation system based on Simulink," 2015 IEEE Energy Conversion Congress and Exposition, Montreal, QC, Canada, 2015, pp. 3265-3270.